Indian Journal of Geo Marine Sciences
Vol. 53 (05), May 2024, pp. 310-321
DOI: 10.56042/ijms.v53i05.21660

Structural design and analysis of a wave energy-based navigational buoy

A Majumdar*, A Vishwanath & P Jalihal

National Institute of Ocean Technology, Chennai, Tamil Nadu – 600 100, India

*[E-mail: anulekha@niot.res.in; anulekha.niot@gmail.com]

Received 30 March 2024; revised 16 May 2024

Ocean has a huge potential to produce electricity from various resources, such as waves, tides, ocean thermal gradient and ocean salinity gradient. Out of these energy sources, wave energy is said to have a higher energy density and smaller fluctuations in power over longer durations compared to other ocean renewables. India has a moderate wave energy potential, but with a long coastline, it can be a potential energy source for the coastal and island communities. The National Institute of Ocean Technology (NIOT) has been working on harnessing this wave energy and has developed many devices for it. Recently, the NIOT team successfully demonstrated an all-weather floating buoy in the waters of Kamarajar Port, Chennai, for powering a beacon lamp on top of the buoy and oceanographic-related components using energy extracted from the ocean waves. While powering the beacon, this navigational buoy will be subjected to various waves, currents, winds and mooring loads. All the buoy parts should be strong enough to withstand the loads. The buoy was designed and analysed in ANSYS APDL for extreme load conditions and was found to be structurally sound. The inertia relief feature available in the software was explored, and the results were compared with those obtained using the standard method for solving similar problems. This paper provides an overview of the wave energy landscape in India. It details the development of this indigenous wave-powered navigational buoy, highlighting its design, testing, and applications in supporting maritime navigation and oceanographic research.

[**Keywords**: Finite Element Analysis (FEA), Indian wave energy scenario, Navigational buoy, Oscillating water column (OWC), Wave energy]

Introduction

In recent decades, there has been a gradual shift towards exploring and utilising renewable energy sources. Wave energy is a renewable resource with a very high energy density compared to other forms of renewable energy. Out of the total renewable energy available worldwide, wave energy potential is 3 TW(ref. 1). However, it is still in the early stages of development due to its short-term fluctuations. Wave potential is available in abundance in mid-latitudes of 40 – 60°, both in the northern and southern hemispheres[2]. Figure 1 shows the global distribution of the maximum significant wave height over a decade.

Tropical locations, like India, have a maximum of 29 kW/m potential[4]. Though lower than higher latitudes, it is an important resource since designing offshore devices for such energy sources is much easier compared to other ocean renewables. The first wave energy plant in India was set up in Vizhnijam, Kerala, on the Southern coast[5]. This OWC-based fixed wave energy plant powered a 10000 litres/day Reverse Osmosis (RO) plant. Following its successful demonstration, a few floating Oscillating Water Column (OWC)-based wave energy devices were developed and demonstrated, out of which a floating buoy was developed as a navigational aid in ports and harbours.

The paper presents the method of wave power estimation, followed by the Indian wave energy scenario in the second section. The third and fourth sections discuss various wave energy converters, focusing on the type developed by NIOT. The fifth section details the development of a wave energy-based navigational buoy, including Computational Fluid Dynamics (CFD) and structural analysis. The sixth section describes the sea trials conducted for the buoy. The paper concludes with a discussion and final remarks.

Materials and Methods

Wave energy assessment

Cornett[3] and Gunmark *et al.*[6] calculated the global wave energy potential for 10 years from 1997 to 2006. Gunmark *et al.*[6] took their data from two sources. The first source was World Waves data[7],

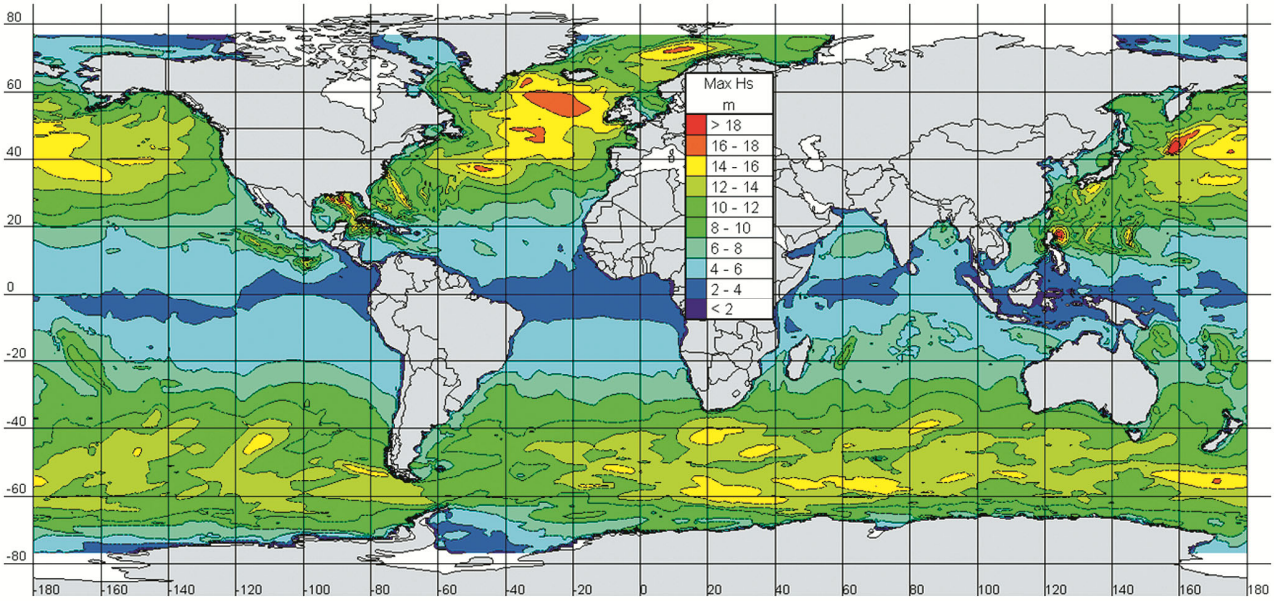

Fig. 1 — Global significant wave height distribution over a decade, from 1997-2006[ref. 3]

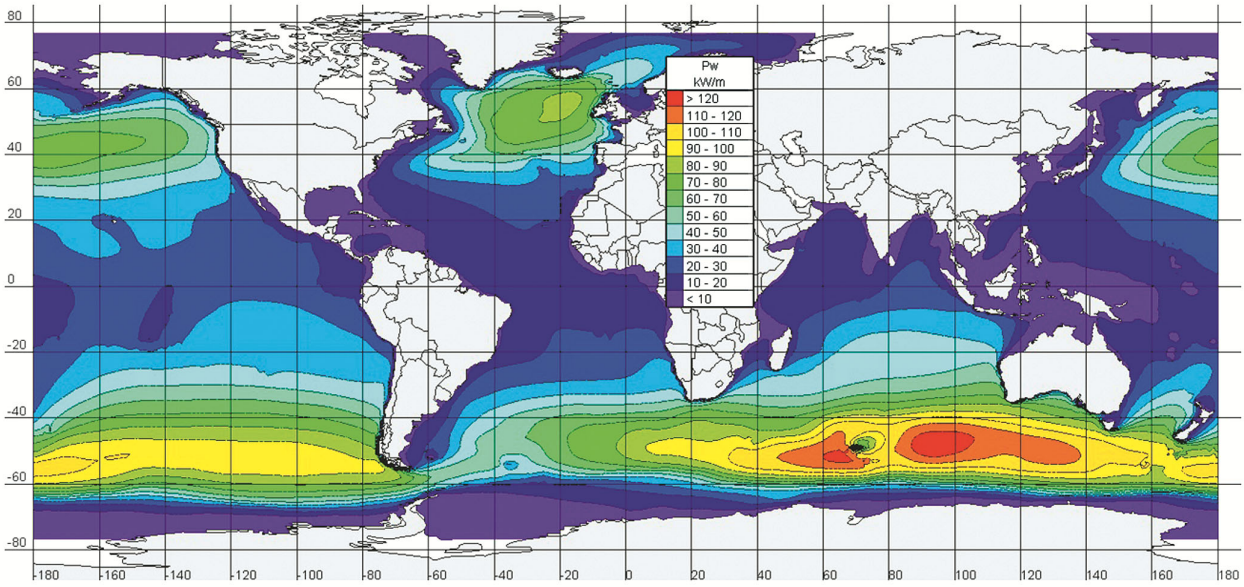

Fig. 2 — Annual mean wave power distribution globally[ref. 3]

consisting of data from the ECMWF WAM model, a 10-year data from 1997 to 2006. This data was cross-verified or validated against satellite altimetry data (TOPEX/JASON). The second source was buoy data, which was used as a final verification step. After comparing the data for the given period, it was observed that there was not much change in the wave period and direction for open sea areas. In contrast, wave periods gradually adjusted according to the wave heights in the closed seas. Cornett[3] took the NOAA Wave Watch III (WW3) global wind-wave model, calibrated it against satellite and buoy data and identified high-energy regions suitable for wave energy exploitation.

In 2012, Gunn *et al.*[8] analysed six-year data (2005 – 2011) from NOAA WW3, and calculated the available power. They used a spatial resolution of 30 arc minutes and a temporal resolution of 3 hours. The method of estimating wave power can be found in Cornett[3] and Gunn *et al.*[8]. The plots obtained from these studies displayed a good match with buoy measurements. Figure 2 shows the plot obtained by

Table 1 — Development of wave energy converters in east and Southeast Asian countries[24]

Country	Project name	WEC	Capacity [kW]
South Korea	Caisson-type oscillating water column wave energy conversion devices	OWC	500
China	"Hai Ling" wave energy recorder buoy	OWC	0.06*2
Japan	Mighty whale	OWC	110
China	Jellyfish type WEC	OB	10
China	"Wanshan" Sharp eagle WEC	OB	120
China	Sharp eagle offshore mobile WEC platform	OB	500

*OWC: Oscillating Water Column, OB: Oscillating Body

Gunn *et al.*[8]. It is evident from the plot that maximum wave power potential occurs between 40 – 60° latitudes and more in the southern hemisphere, near Australia.

Significant development has been made in South East Asia to extract power from the waves. Table 1 shows the summary of the development of wave energy converters in East and Southeast Asian countries.

Indian wave scenario

India has an average wave potential of about 5 – 15 kW/m. However, with a vast coastline of about 11098 km(ref. 9), wave energy becomes a potential source for coastal cities and islands. Sannasiraj & Sundar[4] analysed the wave climate of the Indian coast and concluded that the Indian coast has a wave potential of 40 GW. The southern tip of India has a higher wave potential of around 20 kW/m. Amrutha *et al.*[10] investigated the potential of the wave along the Indian coast using 40 years of data from 1978 to 2018. They concluded that the western locations in India have a slightly higher increase in trend of power generation, a 0.024 kW/m per year increase, compared to the eastern coast, which stands at 0.015 kW/m per year increase in wave power generation. It was also observed by both Sannasiraj & Sundar[4] and Amrutha *et al.*[10] that the wave power is highest during the southwest (SW) monsoon period. Many studies have been carried out to assess the wave energy potential.

Classification of Wave Energy Converters (WEC)

Wave energy converters can be broadly classified based on their fixity, their distance from the shore and their position relative to mean sea level.

A. Based on fixity

Based on the fixity of the system, WEC can be classified as fixed type or floating type WEC.

Fixed WEC

Fixed WECs are devices integrated with any land protection structure, such as breakwaters. The most common type is breakwater-based Oscillating Water Columns (OWC). Figure 3 shows a typical fixed-type WEC based on the OWC principle, commissioned in Vizhinjam, India. These WECs do not require any moorings.

Fig. 3 — Fixed type WEC in Vizhinjam(ref. 11)

Floating WEC

These constitute devices that are not associated with any supporting structure. These WECs are held in a place with the help of moorings. Figure 4 shows a floating wave energy device developed by NIOT.

B. Based on the distance from the shore

Onshore WEC

The devices on the shore or attached to the shore are called onshore devices. The Vizhinjam wave energy plant can be classified as an onshore WEC.

Nearshore WEC

The devices in shallow water within 20 m of water depth[13] are called nearshore devices. The OSPREY OWC(ref. 14) were classified as nearshore devices.

Fig. 4 — Backward Bent Ducted Buoy (BBDB) developed by NIOT[ref. 12]

Offshore WEC

Devices deployed in deep water (*i.e.*, D/L > 0.5, where D is the water depth and L is the wavelength) are called offshore devices. Pelamis WEC[ref. 15] can be classified as an offshore WEC.

C. Based on position with respect to Mean Sea Level (MSL)

Surface following WECs

The WECs partially above the mean sea level are classified as floating WECs. They follow the wave motion. Backward Bent Ducted Buoy (BBDB)[12] and wave-powered navigational buoy developed by NIOT are a few examples.

Submerged WECs

The WECs not visible above the water level or can be fully submerged in water are termed submerged WECs. The Archimedes Wave Swing (AWS), a submerged point absorber[16] and Oyster, a submerged oscillating wave surge converter[17], are examples.

Wave energy devices developed by NIOT

The Indian wave energy program was devised in the eighties at the Indian Institute of Technology (IIT) Madras. NIOT has spearheaded the development of wave energy devices since its advent in 1994. NIOT developed three distinct devices: (a) A wave energy plant at Vizhinjam (a project started by IIT Madras and later taken over by NIOT), (b) A backward bent ducted wave energy buoy to power small loads, and (c) A wave-powered navigational buoy. All these employ the OWC technique for harnessing energy in waves. In an OWC, a chamber is open to the sea below the water level. As waves move, the water level inside the chamber rises and falls, which pressurises the air above. This pressurised air is then forced through an aperture at the top of the chamber, driving a turbine connected to an electric generator, thereby producing electricity.

The pilot wave energy plant in India was an OWC-based fixed WEC. This plant is located in Vizhinjam, Kerala, at 10 m water depth and has the potential to produce an annual average of 15 kW/m of power. A reverse osmosis plant of 10000 litres/day was installed in 2003. The RO was run using the power generated from the wave energy plant. The plant was decommissioned after successful demonstration. Following the successful demonstration of the wave energy plant, a floating BBDB, based on the same principle, was developed and demonstrated in Kamarajar port in 2011. The power module on BBDB consisted of a Unidirectional Impulse (UDI) turbine and a Permanent Magnet Direct Current (PMDC) generator. The turbine designed for the BBDB was utilised in the wave-powered navigational buoy developed for watchkeeping in the ports[18].

Development of an indigenous wave-powered navigational buoy

Yoshio Masuda developed Japan's earliest wave energy converter-based navigational buoy based on the principle of OWC[ref. 19]. The wave-powered navigational buoy developed by NIOT utilises the same principle to convert wave power to electricity. A floating body and oscillating water column within the structure attains primary wave energy conversion. The wave-powered navigational buoy developed was of similar size to that of the conventional solar-powered navigational buoy. The power generated from the waves is used to charge a battery, which then powers the loads connected to it, such as a beacon lamp and other oceanographic instruments. The power requirement for such buoys is very low, thus making it suitable for coasts with milder to lower wave climates.

Numerical analysis of the wave-powered navigational buoy

Computational Fluid Dynamics (CFD) analysis

Computational Fluid Dynamics studies were conducted to ascertain the navigational buoy's sizing and performance[20]. Numerical wave-load models using two-phase Navier-Stokes equations were employed to assess the dynamic wave forces acting on the structure. The RANS-based computational fluid dynamics method, incorporating the free-surface

Volume of Fluid (VOF) multiphase flow was used to calculate the forces on the buoy and its resulting motion in two Degrees of Freedom (DOF). A comparative study was carried out to determine the optimum diameter of the OWC out of 0.9 m and 1.1 m. A regular wave height of 0.8 m and a time period of 4.4 seconds was considered. The draft of the system was 3.6 m. The buoy's movement was analysed utilising the Dynamic Fluid Body Interaction (DFBI) morphing mesh technique. STAR CCM + CFD-based solver was used for this. The simulation gave a pressure field in the 3D domain, motion of the buoy, volumetric flow rate and velocity. The power was then derived by integrating the dot product of the pressure, and the velocity over the surface was obtained following the equation

$$P(t) = \int (p.u) dA \quad \ldots (1)$$

Where, $P(t)$ is the instantaneous power at any given time, t, p is the pressure field, u is the velocity field, and A is the cross-sectional area of the OWC chamber.

Figure 5 shows the domain of the buoy. The domain was 100 m long, 12 m wide and 30 m high. An overset block of 6 m × 6 m × 9 m was selected to capture the relative motion of the buoy with respect to the water plane.

It was observed that the 1.1 m diameter buoy produced 43 % more power than the 0.9 m diameter buoy, as shown in Figure 6. Figure 7(a – d) show the motions, the pressure drop and the volumetric flow rate obtained for the buoy with 1.1 m OWC chamber diameter.

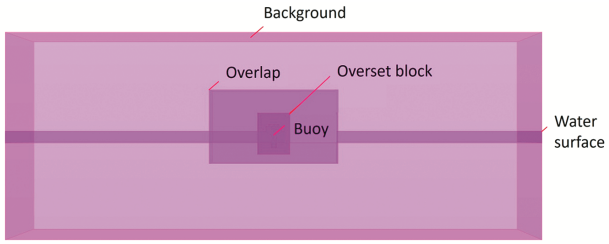

Fig. 5 — Model domain in STAR- CCM+

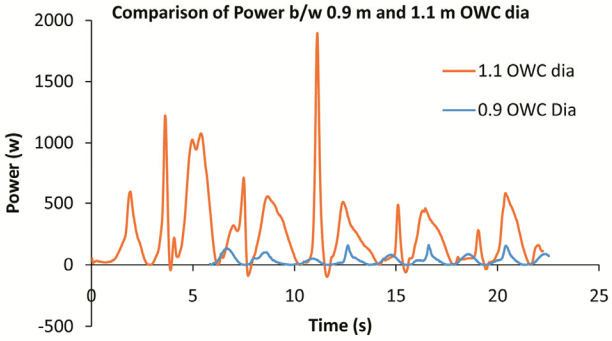

Fig. 6 — Power obtained for 0.9 m and 1.1 m diameter of OWC[ref. 20]

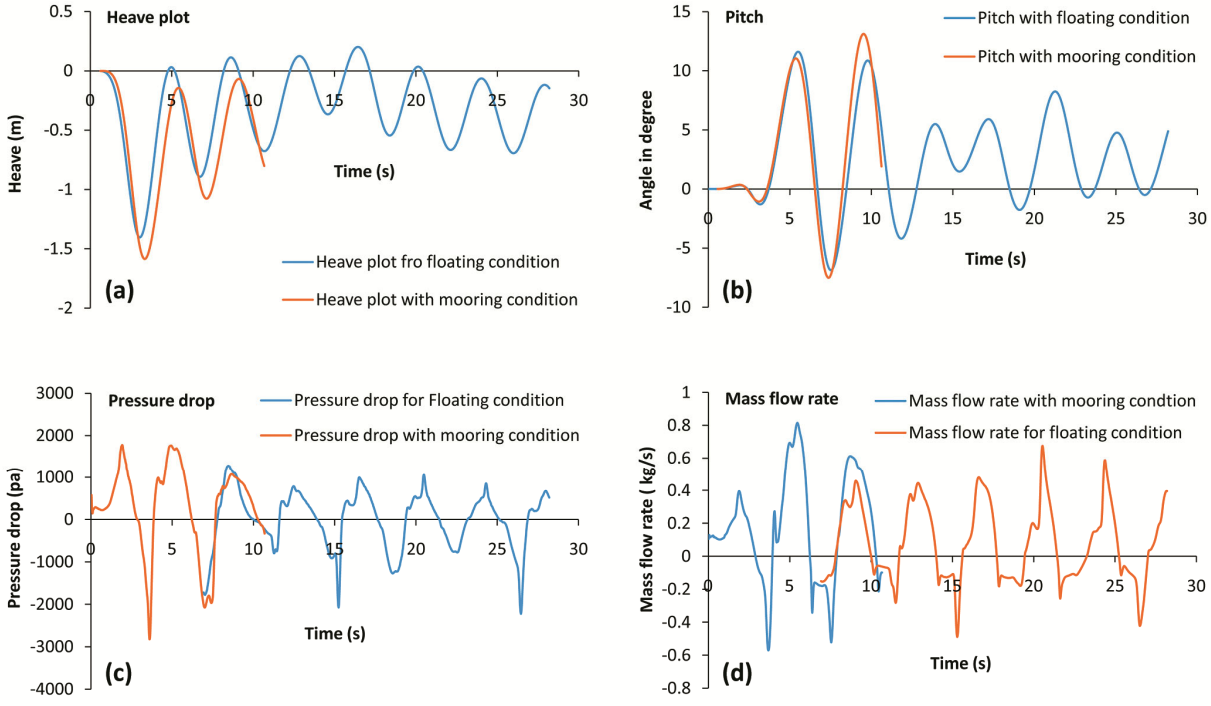

Fig. 7 — (a) Heave, (b) Pitch, (c) Pressure drop, and (d) Mass flow rate, for floating and moored condition with OWC diameter of 1.1 m

Structural analysis

Following the initial sizing and performance evaluation of the buoy from the CFD studies, a structural analysis was carried out using the Finite Element Analysis (FEA)-based software ANSYS APDL[ref. 21].

Geometry

The navigational buoy has two components: the floating buoy and the spar. The buoy is responsible for floating the system, and the spar houses an air turbine responsible for generating electricity from the waves. The buoy used here had a diameter of 3 m and a length of 1.3 m. The spar was 4.8 m long with a diameter of 1.1 m. A bulb flat stiffener, which is a combination of a plate stiffener with a rounded bulb along one edge, was used on the inner face of the buoy to provide sufficient strength against wave loads. Bulb flat stiffeners are commonly incorporated in the hulls of ships. They offer various advantages over simple plate stiffeners, such as higher buckling resistance due to increased strength-to-weight ratio, higher corrosion resistance, simplicity, and ease of welding and painting. Figure 8 shows the navigational buoy, and Table 2 shows the different dimensions of the buoy.

Material selection

The material selected for the buoy was steel due to the ease of availability and machining. The mechanical properties of steel used in the analysis are shown in Table 3.

Pre-processing

The navigational buoy was modelled using the FEA software ANSYS APDL. The buoy was modelled using 2D elements to reduce the computation time. SHELL 181 was used for the hull. BEAM 188 element was used to model the stiffeners. A hexahedral mesh size of 50 mm was selected based on the grid independence test, with the structure having 11390 elements. Figure 9 shows the shell model and mesh of different components made in APDL.

Boundary conditions

Since the buoy will freely float in water, the fixed boundary condition was given so that minimum points are fixed. Here, only four nodes at each hook were fixed. A case using inertia relief was also performed to compare the results of the two cases. Inertia relief applies to floating bodies, such as ships, buoys, and aeroplanes, where the body is in equilibrium even though it is not constrained. For such bodies, ANSYS APDL has a command to switch on the inertia relief and provide minimum constraints to prevent rigid body motion. These constraints should preferably be closer to the body's center of gravity (CoG) to improve simulation accuracy by minimising

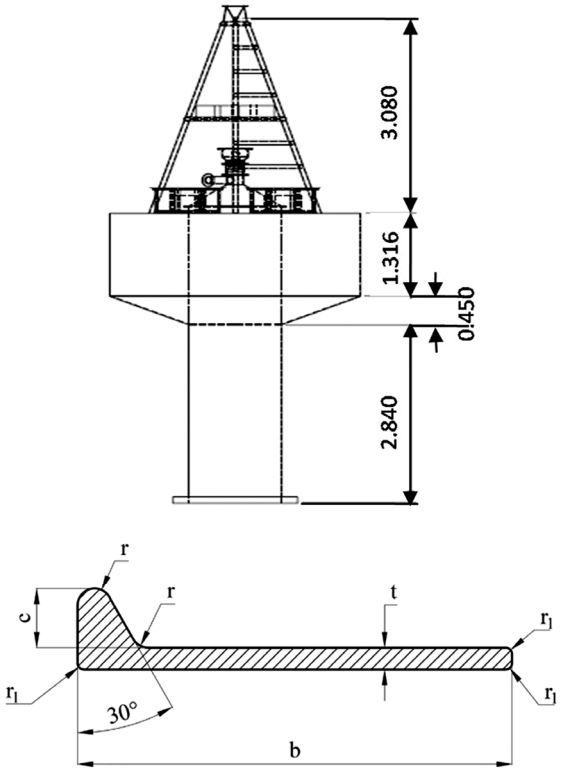

Fig. 8 — Navigational buoy dimensions and a typical bulb flat configuration

Table 2 — Dimensions of various buoy components

OWC specifications	
Diameter	1.1 m
Length	4.8 m
Hull specifications	
Diameter	3 m
Length	1.3 m
Length of the truncated portion	0.5 m
Bulb flat Stiffener specifications	
Breadth (*b*)	80 mm
Thickness (*t*)	6 mm
Number of stiffeners	12

Table 3 — Mechanical properties of steel

Property	**Structural steel**
Density (kg/m^3)	7850
Young's modulus (GPa)	200
Poisson's ratio	0.3
Yield strength (MPa)	250

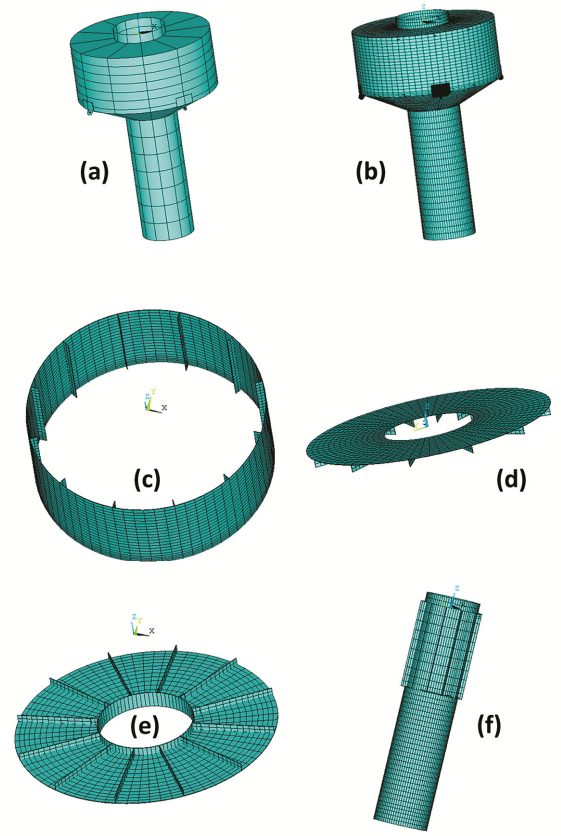

Fig. 9 — (a) Navigational buoy modelled using shell element; (b) Meshing of the structure; (c) Navigational buoy chamber; (d) Top cover of buoy; (e) Bottom cover of buoy; and (f) OWC

numerical errors, ensuring balanced load distribution, and enhancing convergence, as when inertia relief is applied at the CoG, it closely matches the real physical behaviour of the body under loading conditions. This help balance the forces and moments more effectively, minimising numerical errors that could arise from imbalances. This step is crucial for achieving a stable and convergent solution in FEA.

Load calculations

Computing the loads on a slender body, such as a buoy designed for a coastal area prone to cyclonic conditions, involves evaluating the combined effects of drag force, current force, and hydrostatic force. In cyclonic conditions, wave heights can reach up to 10 m within an 11.3-seconds period, and wind speeds can soar to 55 – 60 m/s. These extreme conditions resulted in an overall load of 50 kN/m² calculated from drag pressures, the prevailing currents of 1 m/s and the hydrostatic pressure. A mass of 600 kg, equivalent to 5.89 kN, was applied at the bottom of the buoy, ensuring it remained in stable equilibrium at

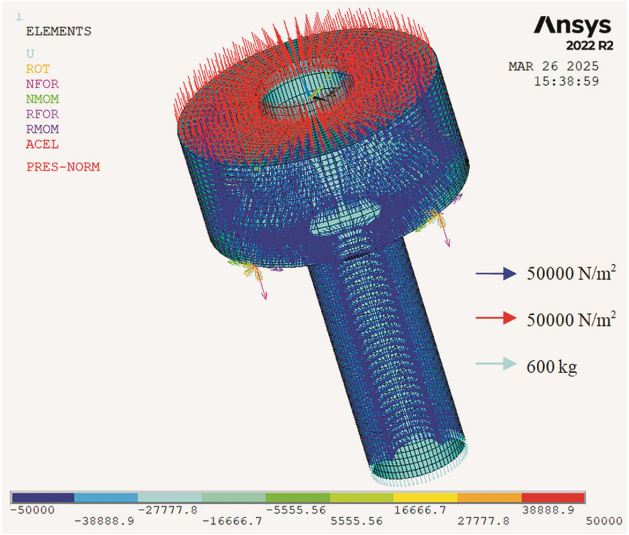

Fig. 10 — Loads applied on the buoy

all times. Figure 10 shows the loads applied to the structure.

The following loads were applied to the structure

1. 50 kN/m^2 of the top cover
2. 50 kN/m^2 on the hull
3. 600 kg at the bottom of the buoy

Results

Buoy hull

The structure was analysed for the above boundary conditions with the following load combinations. The structure should not go beyond the yield limit of the material for it to be in usable condition. The failure criteria for checking the structure's integrity is von Mises stress. von Mises stress is used to predict the yield point of ductile materials. It provides an equivalent stress value that combines all the individual stress components, tensile, compressive and shear stresses into a single scalar value. This simplifies the analysis of complex stress states.

Case 1: Load of 50 kN/m^2 applied on the hull, OWC and top cover, 600 kg at the bottom of the OWC of the buoy, nodes of hook fixed. Figure 11 shows that the maximum von Mises stress is around 112 MPa, and the maximum deformation occurring on the top cover of the buoy is 3.5 mm.

Case 2: Load of 50 kN/m^2 applied on the hull, OWC and top cover, 600 kg at the bottom of the OWC of the buoy, inertia relief enabled. Figure 12 shows that the maximum von Mises stress is around 103 MPa, and the maximum deformation occurring on the top cover of the buoy is 3.1 mm.

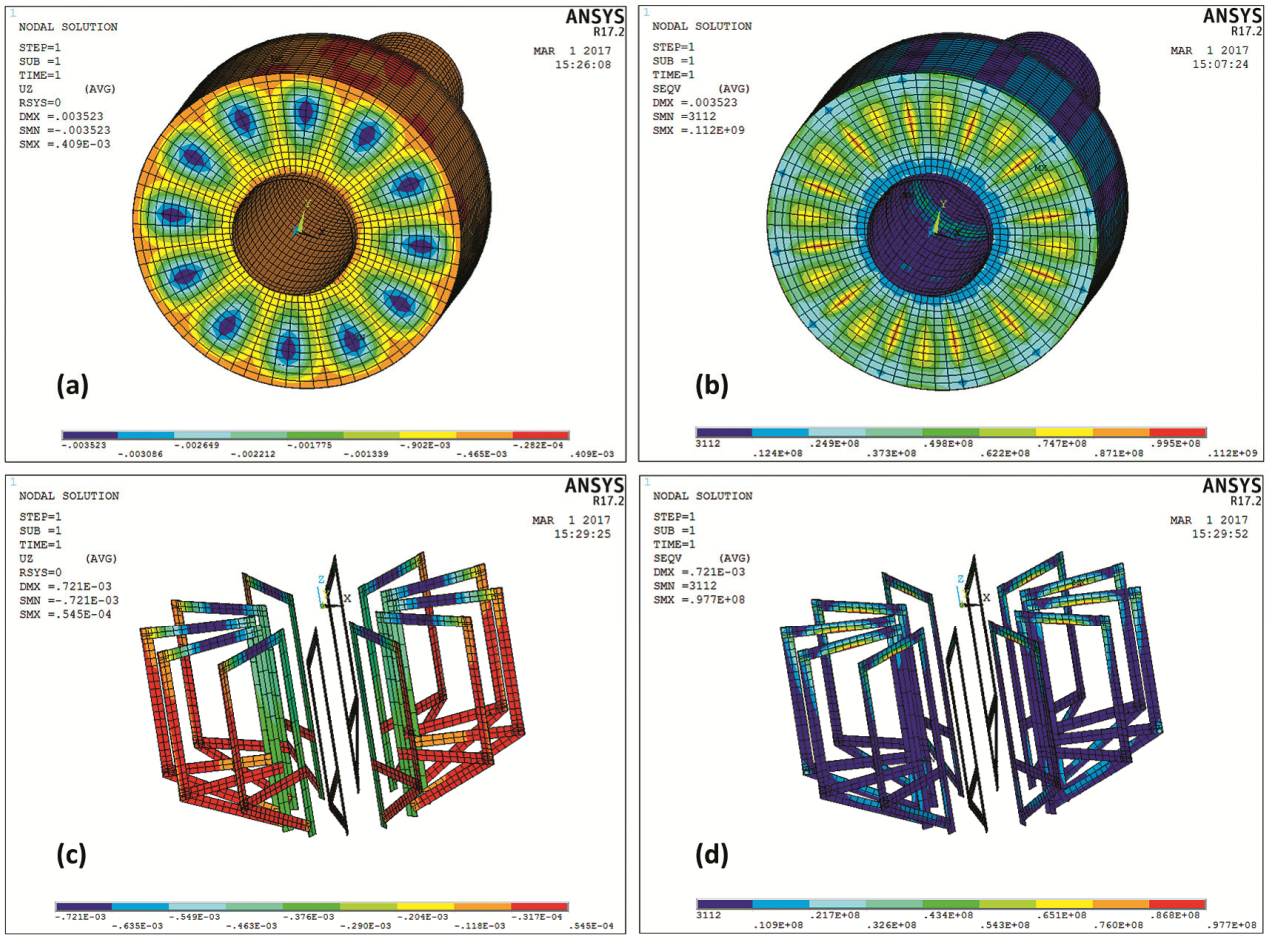

Fig. 11 — Case 1: (a) Deformation contour of the buoy; (b) Stress contour of the buoy; (c) Deformation of bulb flat stiffener; and (d) Stress on bulb flat stiffener

For both load cases, the maximum von Mises stress occurs on the top cover at the locations where stiffeners are placed. The maximum deformation occurs on the top cover at a place located between two consecutive stiffeners.

Pad eye

A pad eye is a type of hardware used in various applications to provide a secure anchor point for attaching ropes, cables, chains, or other fittings. It typically consists of a flat metal plate with a loop or eyelet protruding from it. The pad eye used for mooring purposes was also checked for stresses. Figure 13 shows the geometry of the pad eye used in the analysis. The dimensions of the pad eye are presented in Table 4.

A load of 100 kN was applied to the pad eye, and the stress and deformation values were checked. The horizontal face of the pad eye was given a fixed support. Figure 14 shows the maximum effective tension in the mooring line obtained from mooring analysis carried out using Orcaflex software. The maximum von Mises stress was found to be 52.8 MPa at the bottom of the circular hole, and the deformation was negligible, as shown in Figure 15.

Sea trials

After the design was completed, the buoy was fabricated and tested in the open sea. During several sea trials, the buoy was deployed off the coast of Chennai, close to the south navigational channel of the Ennore port[22]. The components of the buoy hull, including the buoyancy hull, OWC, and ballast weights, were assembled at the port jetty and lowered into the calm water alongside the jetty. Power modules, instruments, and antennae were integrated into the buoy. Subsequently, tug boats towed the buoy to its designated location. Figure 16 illustrates the buoy being towed and its final position in the sea.

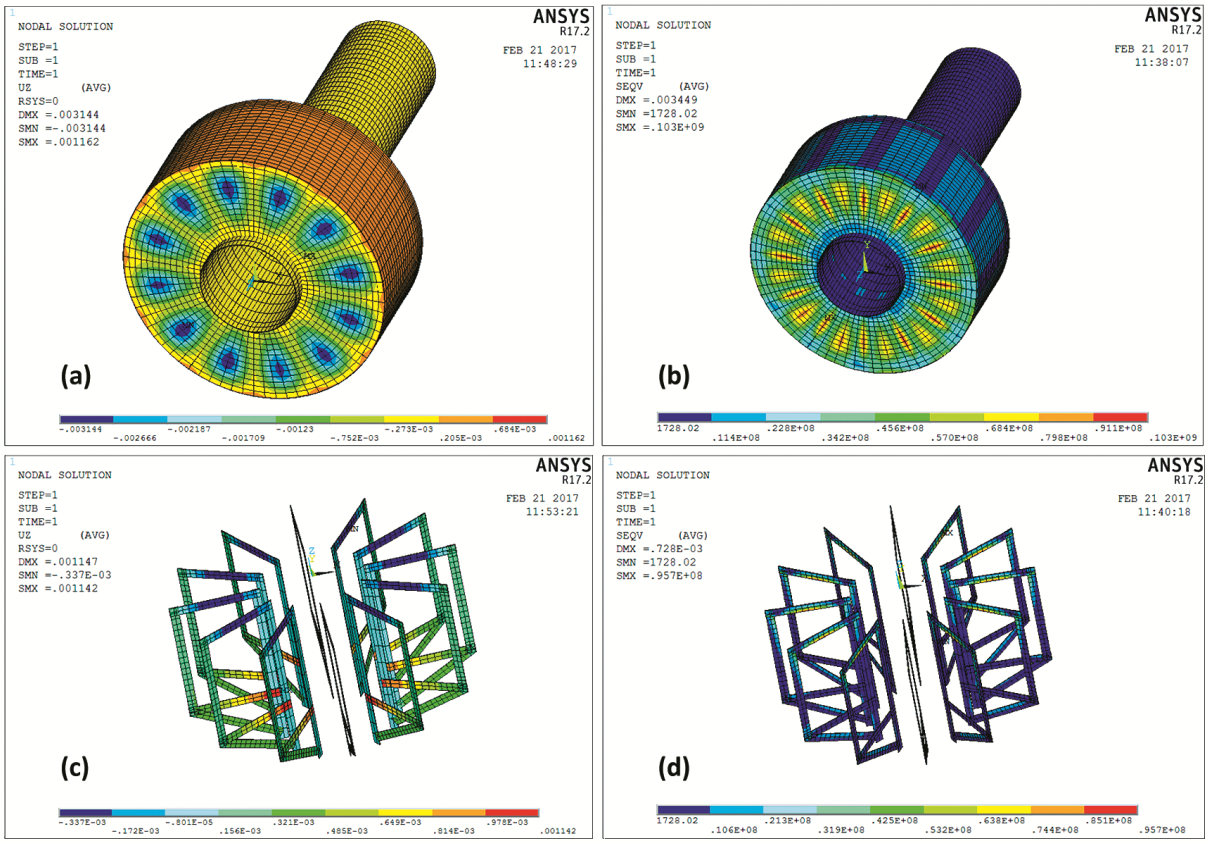

Fig. 12 — (a) Deformation contour of the buoy; (b) Stress contour of the buoy; (c) Deformation of bulb flat stiffener; and (d) Stress on bulb flat stiffener

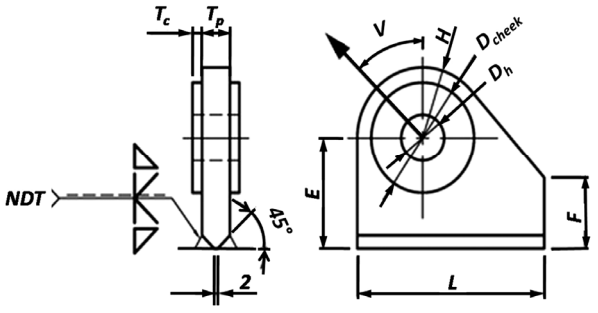

Fig. 13 — Pad eye geometry

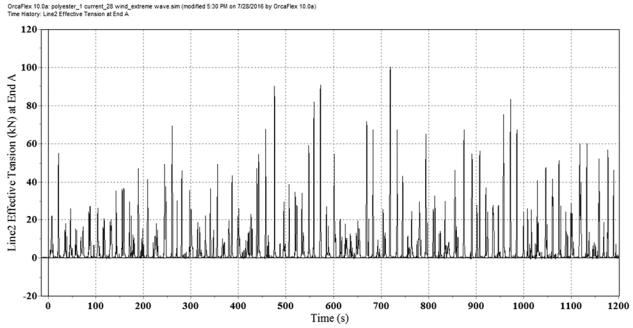

Fig. 14 — Effective tension in the mooring line

Table 4 — Pad eye dimensions

D_h	50 mm
F	75 mm
E	125 mm
L	280 mm
T_p	40 mm

The buoy electrical power budget included marker lamps, sensors, and data loggers. The data logger consumed 47 % of the total power, and all other sensors, including the lamp, consumed the rest.

Oceanographic instruments like the wind monitor sensor and Doppler current sensor were used to record the data continuously with the help of a designed embedded system. The same data was transmitted to the FTP server using GSM communication. These recorded data were processed in MATLAB to draw wind rose diagrams to understand the wind and current movement in a meteorological sense. The wind speed, current speed and the direction depend highly on local topography and climate conditions.

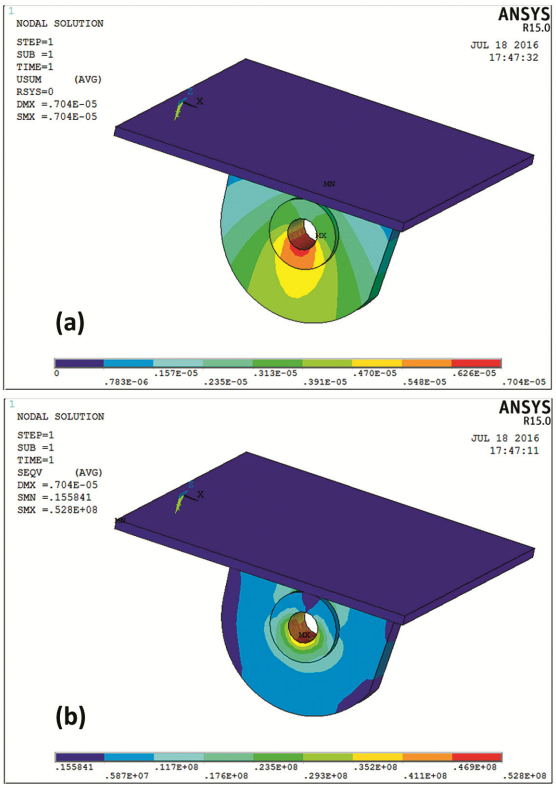

Fig. 15 — (a) Deformation in pad eye; and (b) Stress in pad eye

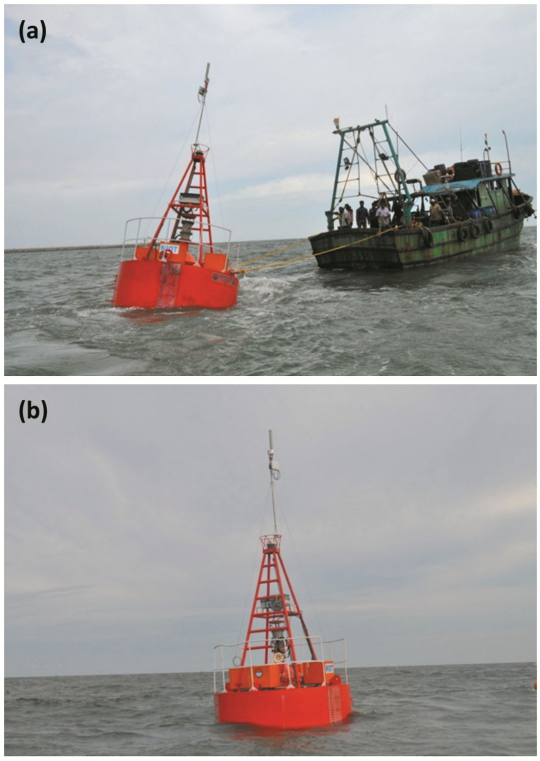

Fig. 16 — (a) Towing of the buoy to the site; and (b) In-place position of the buoy

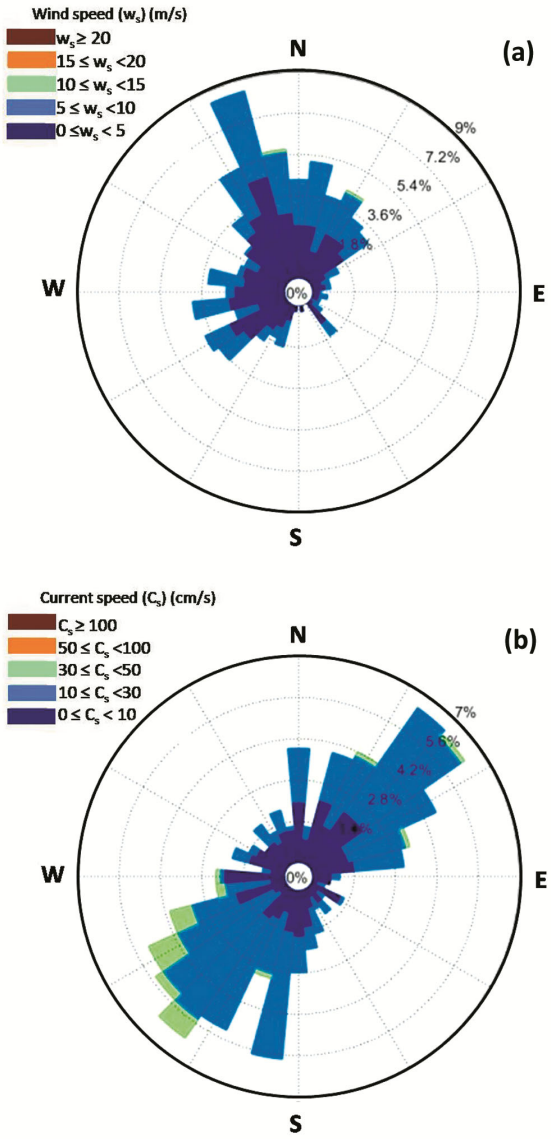

Fig. 17 — (a) Wind rose plot from measured data transmitted by the buoy; and (b) Current rose plot from measured data transmitted by the buoy

Figure 17 shows the rose diagrams plotted from a typical month's recorded wind and current sensors.

Discussion and Conclusion

A summary of the results is presented in Table 5. From the first two cases, it can be seen that the difference between the case without inertia relief and the case with inertia relief is about 8 %, which is very small. Also, as the yield strength of the material is 250 MPa, a factor of safety of more than 2 was obtained for all the load conditions. For marine applications, a safety factor between 1.5 – 3 is acceptable[23], and hence the design is deemed safe.

Table 5 — Summary of results obtained from structural analysis of buoy

Sl. No.	Case	von Mises stress (MPa)	Deformation (mm)	Factor of safety
1	Load of 50 kN/m^2 applied on the hull, OWC and top cover, 600 kg at the bottom of the OWC of the buoy, nodes of hook fixed	112	3.5	2.23
2	Load of 50 kN/m^2 applied on the hull, OWC, and top cover, 600 kg at the bottom of the OWC of the buoy, inertia relief enabled	103	3.1	2.42
3	A load of 10 tons applied on the pad eye with fixed top surface	52.8	0.07	4.73

The article presents the wave energy potential available in India, and the various devices that can be used for wave energy conversion. Article further discusses the development of wave energy devices in NIOT, which paved the way for developing a floating wave energy device for powering navigational and observational instruments for usage in ports/harbours through a series of studies involving numerical and sea trials. All the sub-components of the complete buoy system, including the communication system, were designed in-house. The paper discusses the FEA carried out to design and develop the structure of the navigational buoy. Two kinds of analyses were carried out: one with nodes of eye hook fixed and another inertia relief to model such floating components with minimum constraints. It was found that for both cases, a factor of safety of more than 2 was obtained for an extreme wave condition of 10 m wave height and 11.3 seconds period. The pad eye was separately checked for its structural integrity by applying a load of 100 kN, and it was found to have safety factor of more than 4. The buoy system underwent several sea trials, and measured data from the wave-powered sensors were transmitted to port authorities hourly.

Acknowledgements

The authors would like to thank the Ministry of Earth Sciences, Government of India, for its support.

Conflict of Interest

The authors declare that they have no known competing or conflict of interest.

Author Contributions

AM: Conceptualization, writing - original draft, formal analysis, and visualization. AV: Writing - review & editing, visualization, and supervision. PJ: Conceptualization, writing - review & editing, visualization, and supervision.

References

1 Twidell J, *Renewable Energy Resources*, 4th edn, (Routledge, London), 2021, pp. 774. https://doi.org/10.4324/9780429452161

2 Centre for Renewable Energy Sources (CRES), *Wave Energy Utilization in Europe: Current Status and Perspectives*, (Pikermi, Greece), 2002, pp. 32.

3 Cornett A M, A Global Wave Energy Resource Assessment, In: *The Eighteenth International Offshore and Polar Engineering Conference*, Vancouver, Canada, July 2008, 2008, pp. 1-9.

4 Sannasiraj S A & Sundar V, Assessment of wave energy potential and its harvesting approach along the Indian coast, *Renew Energy*, 99 (2016) 398–409. https://doi.org/10.1016/j.renene.2016.07.017

5 Sharmila N, Jalihal P, Swamy A & Ravindran M, Wave powered desalination system, *Energy*, 29 (11) (2004) 1659–1672. https://doi.org/10.1016/j.energy.2004.03.099

6 Mørk G, Barstow S, Kabuth A & Pontes M T, Assessing the Global Wave Energy Potential, In: *29th International Conference on Ocean, Offshore and Arctic Engineering*, Vol 3, ASMEDC, Jan. 2010, 2010, pp. 447–454. https://doi.org/10.1115/OMAE2010-20473

7 Barstow S F, Mørk G, Lønseth L, Schjølberg P, Machado U, *et al.*, WORLDWAVES: High Quality Coastal and Offshore Wave Data Within Minutes for Any Global Site, In: *Materials Technology; Ocean Engineering; Polar and Arctic Sciences and Technology; Workshops*, 3, 2003, ASMEDC, pp. 633–642. https://doi.org/10.1115/OMAE2003-37297

8 Gunn K & Stock-Williams C, Quantifying the global wave power resource, *Renew Energy*, 44 (2012) 296–304. https://doi.org/10.1016/j.renene.2012.01.101

9 TRW: Transport Research Wing, Change in length of coastline of India (Circular), Ministry of Ports, Shipping and Waterways (MoPSW), Government of India, New Delhi, Dated 29 April 2025, 2025, pp. 03. https://www.shipmin.gov.in/sites/default/files/Length%20of%20Indias%20Coastline%20Circular.pdf

10 Amrutha M M & Kumar V S, Changes in Wave Energy in the Shelf Seas of India during the Last 40 Years Based on ERA5 Reanalysis Data, *Energies (Basel)*, 13 (1) (2019) p. 115. https://doi.org/10.3390/en13010115

11 Sharmila N, Jalihal P, Swamy A & Ravindran M, Wave powered desalination system, *Energy*, 29 (11) (2004) 1659–1672. https://doi.org/10.1016/j.energy.2004.03.099

12 Pattanaik B, Nagasamy D, Karthikeyan A, Leo D, Narasimha Rao Y V, *et al.*, Open sea trials on floating wave energy device backward bent ducted buoy and its performance optimisation, In: *Proceedings of the Fourth International Conference in Ocean Engineering (ICOE2018)*, edited by

Murali K, Sriram V, Samad A & Saha N, (Springer, Singapore), 2019, pp. 775–791. https://doi.org/10.1007/978-981-13-3134-3_58

13 Thorpe T W, An overview of wave energy technologies: Status, performance and costs, In: *Wave Power: Moving Towards Commercial Viability*, 30 November 1999, Broadway House, Westminster, London, (Wiley, US), 1999, pp. 50-120.

14 Kingston W, Examining the Effectiveness of Support for UK Wave Energy Innovation since 2000. Lost at Sea or a New Wave of Innovation? *Prometheus*, 35 (2) (2017) 145-158. https://doi.org/10.1080/08109028.2018.1486534

15 Frandsen J B, Doblaré M, Rodríguez P & Reyes M, *Technical assessment of the Pelamis Wave Energy Converter concept*, 2012, pp. 283.

16 Heath T, Sarmento A, Neumann F, e Melo A B, Prado M, *et al.*, Full-Scale WECs, In: *Ocean Wave Energy: Current Status and Future Prespectives*, edited by Cruz J, (Springer, Berlin Heidelberg), 2008, pp. 287–395. https://doi.org/10.1007/978-3-540-74895-3_7

17 Whittaker T, Collier D, Folley M, Osterried M, Henry A, *et al.*, The development of Oyster - a shallow water surging wave energy converter, In: *7th European Wave and Tidal Energy Conference*, Porto, Portugal, Sep. 2007, 2007, pp. 11-14.

18 Majumdar A, Dudhgaonkar P & Jalihal P, Structural Modification and Optimisation of $AlSi_7$ $Mg_{0.6}$ Alloy Based Rotor for Wave Energy Harvesting, In: *2022 IEEE 7th International Energy Conference (ENERGYCON)*, Riga, Latvia: IEEE, May 2022, 2022, pp. 1–6. https://doi.org/10.1109/ENERGYCON53164.2022.9830359

19 Masuda Y, An Experience of Wave Power Generator through Tests and Improvement, In: *Hydrodynamics of Ocean Wave-Energy Utilization*, edited by Evans D V & Falcao A F O, (Springer Berlin Heidelberg), 1986, pp. 445–452. https://doi.org/10.1007/978-3-642-82666-5_36

20 Vishwanath A, Awasthi N, Jalihal P & Dudhgaonkar P, Performance Simulation of Wave-Powered Navigational Buoy Using CFD and Experimental Study, In: *Proceedings of the Fourth International Conference in Ocean Engineering (ICOE2018)*, Vol 2, edited by Murali K, Sriram V, Samad A & Saha N, (Springer, Singapore), 2019, pp. 869–882. https://doi.org/10.1007/978-981-13-3134-3_64

21 ANSYS Inc., *ANSYS Mechanical APDL Element Reference 14.0*, 2011. https://www.mm.bme.hu/~gyebro/files/vem/ansys_14_element_reference.pdf

22 Pattanaik B, Rao Y V N, Leo D & Jalihal P, Experimental Studies on Development of Power Take Off System for Wave Powered Navigational Buoy, In: *2018 IEEE 13th International Conference on Industrial and Information Systems (ICIIS)*, IEEE, Dec 2018, 2018, pp. 367–370. https://doi.org/10.1109/ICIINFS.2018.8721393

23 DNV GL AS, *Rules for Classification: Ships, DNV GL-RU-SHIP - Part 3: Hull, Chapter 3: Structural design principles*, 2015, pp. 94.

24 Li M, Luo H, Zhou S, Senthil Kumar G M, Guo X, *et al.*, State-of-the-art review of the flexibility and feasibility of emerging offshore and coastal ocean energy technologies in East and Southeast Asia, *Renew Sustain Energy Rev*, 162 (2022) p. 112404. https://doi.org/10.1016/j.rser.2022.112404